Richa Sharma

EVALUATION OF THERMAL ELASTIC-PLASTIC STRESSES IN TRANSVERSELY ISOTROPIC DISK MADE OF PIEZOELECTRIC MATERIAL WITH VARIABLE THICKNESS AND VARIABLE DENSITY SUBJECTED TO INTERNAL PRESSURE

ODREĐIVANJE TERMIČKIH ELASTOPLASTIČNIH NAPONA U TRANSVERZALNO IZOTROPNOM DISKU OD PIEZOELEKTRIČNOG MATERIJALA PROMENLJIVE DEBLJINE I GUSTINE KOJI JE OPTEREĆEN UNUTRAŠNJIM PRITISKOM

Originalni naučni rad / Original scientific paper
UDK /UDC:

Rad primljen / Paper received: 11.11.2022

Adresa autora / Author's address:
Department of Mathematics, Jaypee Institute of Information Technology, Noida (UP), India
email: richa.ggit@gmail.com , richa.sharma@mail.jiit.ac.in

Keywords

- transversely isotropic materials
- functionally graded materials
- piezoelectric materials
- PZT4
- $BaTiO_3$

Abstract

Piezoelectric materials have several packages in engineering and scientific fields. Piezoelectricity is the characteristic of the material due to which the electrical subject is generated in them when mechanical load is applied. PZT4 and $BaTiO_3$ are examples of unnatural piezoelectric substances. In this paper the analytic solution is discussed of thermal stresses in a thin rotating transversely isotropic disk consisting of a piezoelectric with variable thickness and density. Seth's idea of transition is implemented to simplify the governing differential equation. The obtained results are presented graphically and quantitatively. On the idea of evaluation, it is far discovered that a disk made of piezoelectric material barium titanate ($BaTiO_3$) is better than a disk made of PZT4 (piezoceramic). Parameters obtained from this research can be used to design pressure sensors, radar antennae, and many other devices, machines, or structures in engineering applications.

Ključne reči

- transverzalno izotropni materijali
- funkcionalni kompozitni materijali
- piezoelektrični materijali
- PZT4
- $BaTiO_3$

Izvod

Piezoelektrični materijali imaju više primena u inženjerskim i u naučnim oblastima. Piezoelektrični efekat je karakteristika materijala u kojem se stvara električni napon pod dejstvom mehaničkog opterećenja. PZT4 i $BaTiO_3$ su primeri veštačkih piezoelektričnih materijala. U radu je data diskusija o analitičkom rešenju termičkih napona kod tankog rotirajućeg transverzalno izotropnog diska, koji je sačinjen od piezoelektričnog materijala, promenljive debljine i gustine. Ideja Seta o prelaznim naponima je uvedena radi uprošćenja polazne diferencijalne jednačine. Dobijeni rezultati su predstavljeni grafički i kvantitativno. Shodno dobijenim vrednostima, pokazuje se da je disk od piezoelektričnog materijala, barijum titanata ($BaTiO_3$), bolji u odnosu na disk od PZT4 (piezokeramike). Parametri određeni u ovom radu se mogu upotrebiti u projektovanju senzora pritiska, radarskih antena, i u mnogim drugim uređajima, mašinama, ili konstrukcijama u inženjerskoj primeni.

INTRODUCTION

Materials have played an essential position from the early records of mankind. These days piezoelectric substances additionally play an important position in numerous technological packages, which include dental implants and bone implants in scientific subjects and many more. In mid-18th century, Curie brothers verified the existence of the piezoelectric action in quartz, tourmaline, topaz, cane sugar, and Rochelle salt crystals. The first actual application of piezoelectric substances became an ultrasonic submarine detector with the aid of Pierre Langevin in 1917. Piezoelectric substances have splendid importance nowadays and these materials have numerous programmes in extraordinary science and engineering fields. Fuel efficiency of cars is more desirable by piezoelectric fuel injection, airbags are controlled by means of a piezoelectric acceleration sensor and an ultrasonic parking sensor helps in avoiding collisions. Piezo motors are used for MRI monitored microsurgery in hospitals.

Nguyen et al. /1/ added an isogeometric Bézier FE method to perform static bending and brief analysis of piezoelectric (FGP) plates bolstered with the aid of graphene platelets (GPLs). Barati and others /2/ used the polished four-unknown plate technique to study loose vibration of piezoelectric FGM plates with porosities.

To describe the shifting rule of graded material residences of a piezoelectric FGM, a modified electricity-law model was presumptively used. Hamilton's principle-derived governing equations were resolved analytically in a way that satisfied various boundary scenarios. In their study of the free and under pressure vibration of smart FG metal foam plate constructions supported by graphene platelets (GPLs), Nguyen et al. /3/ demonstrated that the proposed method was suitable for modelling both thick and thin structures.

Zharfi et al. /4/ calculated the creep stresses in rotating FGM disc through applying generalised differential quadrature answer method of differential equations. Mathematical model is advanced to analyse regular state creep stresses and

pressure in a variable thickness rotating FGM disc through the use of Tresca yield criterion by way of Khanna et al. /5/. An analytical solution for a polarised circular cylinder, fabricated from piezoelectric FGM was found by Dai et al. /6/, who concluded that FGM have a significant impact. Jafari-Fesharaki et. al. /7/ discussed the analytical solution of a thick, spherical, piezoelectric FGM cylinder subjected to heat and mechanical loads as well as electrical issues. They validated their analytical approach with the aid of solving unique examples by means of this approach. Akbarzadeh et al. /8/ applied the Fourier-Laplace method, it was possible to compute the dynamic response of a functionally graded rectangular plate being subjected to a thermomechanical force. All of the above-cited authors implemented classical theory of deformations for fixing these problems in elastic vicinity, as the simplest.

Using generalised finite strain measures, Borah /9/ has used the notion of the transition principle. Many researchers /10-24/ have carried out the transition principle to solve the problems associated with extraordinary sorts of stable systems together with cylinders, shells and disc and many others, i.e., the stresses in circular cylinder composed of FGM are evaluated by Aggarwal et al. /11/ and determined that functionally graded material is higher in comparison to isotropic material. According to Sharma et al. /17/ analysis of creep torsion in a thick cylinder beneath the impact of pressure at the internal and external surface, composite materials are more advantageous for design.

In the current problem, thermal stresses are calculated in elastic and plastic state in transversely isotropic rotating disk constituted of functionally graded piezoelectric material subjected to inner pressure.

GOVERNING MATHEMATICAL EQUATIONS

A thin rotating disc with radii on the inside and outside as r_1 and r_2, respectively, is taken into consideration and ω is the angular velocity of the disk. The disk considered here is successfully in a plane stress state i.e. ($T_{zz} = 0$). The displacements are taken as

$$u = r(1-\beta);\quad v = 0 \quad \text{and} \quad w = dz\,, \tag{1}$$

where: β is a function of $r = \sqrt{x^2 + y^2}$; and d is constant.

By implementing generalised strain measure, the components of strains are given by

$$e_{rr} = \frac{1}{n}[1-(r\beta' + \beta)^n]\,,\ e_{\theta\theta} = \frac{1}{n}[1-\beta^n]\,,\ e_{zz} = \frac{1}{n}\left[1-(1-d)^n\right],$$
$$e_{r\theta} = e_{\theta z} = e_{zr} = 0\,, \tag{2}$$

where: n is the strain measure and $\beta' = d\beta/dr$.

According to Hook's law

$$T_{rr} = c_{11}e_{rr} + (c_{11} - 2c_{66})e_{\theta\theta} + c_{13}e_{zz} - e_{11}E_r - \beta_1\theta\,,$$
$$T_{\theta\theta} = (c_{11} - 2c_{66})e_{rr} + c_{11}e_{\theta\theta} + c_{13}e_{zz} - e_{12}E_r - \beta_2\theta\,,$$
$$T_{zz} = T_{zr} = T_{r\theta} = T_{\theta z} = 0\,, \tag{3}$$

where: $\beta_1 = \alpha_1 c_{11} + 2\alpha_2 c_{12}$; $\beta_2 = \alpha_1 c_{12} + 2\alpha_2(c_{22} + c_{33})$; α_1 is a coefficient of linear thermal expansion across the axis of symmetry; α_2 is the quantity orthogonal to axis of symmetry; and θ is temperature given by $\theta_0 \log(r/b)/\log(a/b)$; θ_0 is constant.

Electric displacement equations are given as

$$D_r = \in_{11} e_{rr} + \in_{12} e_{\theta\theta} + \in_{13} e_{zz} + \eta_{11}E_r\,,\quad D_\theta = D_z = 0\,, \tag{4}$$

where: c_{11}, c_{66}, c_{13} are material constants; $\in_{11}$, $\in_{12}$, $\in_{13}$ are piezoelectric coefficients; and η_{11} is dielectric constant.

From Eqs.(2) and (4) we have

$$D_r = \frac{C_1}{r} = \frac{1}{r}\,,\quad E_r = \frac{1}{\eta_{11}}\left[\frac{1}{r} - \in_{11} e_{rr} - \in_{12} e_{\theta\theta}\right]. \tag{5}$$

Taking variable compressibility as

$$C_{11} = C_{011}\left(\frac{r}{b}\right)^k,\ C_{12} = C_{012}\left(\frac{r}{b}\right)^k,\ C_{13} = C_{013}\left(\frac{r}{b}\right)^k,$$
$$C_{66} = C_{066}\left(\frac{r}{b}\right)^k. \tag{6}$$

By using Eqs.(3), (4), (5) and (6), stresses are given as

$$T_{rr} = \frac{C_{011}}{n}\left(\frac{r}{b}\right)^k(1-\beta^n(1+P)^n) + \frac{(C_{011}-2C_{066})}{n}\left(\frac{r}{b}\right)^k(1-\beta^n) + \frac{C_{013}}{n}\left(\frac{r}{b}\right)^k(1-(1-d)^n) +$$
$$+\frac{\in_{11}}{n\eta_{11}}\left[\in_{11}(1-\beta^n(1+P)^n) + \in_{12}(1-\beta^n) - \frac{1}{r}\right] - (\alpha_1 C_{011} + 2\alpha_1 C_{012})\left(\frac{r}{b}\right)^k\theta_0\frac{\log(r/b)}{\log(a/b)}\,,$$
$$T_{\theta\theta} = \frac{(C_{011}-2C_{066})}{n}\left(\frac{r}{b}\right)^k(1-\beta^n(1+P)^n) + \frac{C_{011}}{n}\left(\frac{r}{b}\right)^k(1-\beta^n) + \frac{C_{013}}{n}\left(\frac{r}{b}\right)^k(1-(1-d)^n) + \frac{\in_{12}}{n\eta_{11}}\times$$
$$\times\left[\in_{11}(1-\beta^n(1+P)^n) + \in_{12}(1-\beta^n) - \frac{1}{r}\right] - (\alpha_1 C_{012} + \alpha_1(C_{022}+C_{022}))\left(\frac{r}{b}\right)^k\theta_0\frac{\log(r/b)}{\log(a/b)}\,, \tag{7}$$

where: $r\beta' = \beta P$.

The condition of equilibrium for rotating disc is given as

$$\frac{d}{dr}(hT_{rr}) + hT_{\theta\theta} + h\rho\omega^2 r = 0\,. \tag{8}$$

Variable density and thickness are given by

$$\rho = \rho_0\left(\frac{r}{b}\right)^t,\quad \text{and} \quad h = h_0\left(\frac{r}{b}\right)^m. \tag{9}$$

Using Eqs.(7) and (9) in equations in the equilibrium Eq.(8) we have

$$\left(C_{011}\beta^{n+1} + \beta^{n+1}\left(\frac{r}{b}\right)^{-k}\frac{\in_{11}^2}{\eta_{11}}\right)P(1+P)^{n-1}\frac{dP}{d\beta} = (m+k)\frac{C_{011}}{n}(1-\beta^n(1+P)^n) + (m+k)\frac{C_{011}}{n}(1-\beta^n) + \frac{C_{013}}{n}(m+k)(1-(1-d)^n) +$$

$$+\frac{2C_{066}}{n}(1-\beta^n(1+P)^n)-(m+k+1)\frac{C_{066}}{n}(1-\beta^n)+\left(\frac{r}{b}\right)^{-k}\left(\frac{\in_{11}^2(m+1)}{n\eta_{11}}(1-\beta^n(1+P)^n)+\frac{\in_{11}\in_{12}(m+1)}{n\eta_{11}}(1-\beta^n)+\frac{\in_{12}}{r\eta_{11}}-\right.$$
$$\left.-\frac{\in_{11}{}^2}{\eta_{11}}\beta^n P(1+P)^n+\frac{\in_{11}\in_{12}P}{\eta_{11}}-\frac{\in_{12}^2}{\eta_{11}}(1-\beta^n)\right)-(\alpha_1C_{011}+2\alpha_1C_{012})\left(\frac{r}{b}\right)^k\theta_0\frac{\log(r/b)}{\log(a/b)}-(\alpha_1C_{012}+\alpha_1(C_{022}+C_{022}))\left(\frac{r}{b}\right)^k\times$$
$$\times\theta_0\frac{\log(r/b)}{\log(a/b)}+(m+t+2)\frac{\rho_0\omega^2r^{t+1}}{b^t}-C_{011}\beta^nP(1+P)^n \tag{10}$$

The conditions to be implemented are considered as

$$T_{rr}=0 \text{ at } r=b, \text{ and } T_{rr}=-p \text{ at } r=a\,. \tag{11}$$

Conversion from elastic to plastic

As stated by transition theory, conversion from elastic to plastic occurs at critical point $P\to\pm\infty$. The transition function for evaluating the plastic stresses is taken as

$$R=T_{rr}+B+\beta_1\theta=\frac{C_{011}}{n}\left(\frac{r}{b}\right)^k(1-\beta^n(1+P)^n)+\frac{(C_{011}-2C_{066})}{n}\left(\frac{r}{b}\right)^k(1-\beta^n)+\frac{C_{013}}{n}\left(\frac{r}{b}\right)^k(1-(1-d)^n)+\frac{\in_{11}}{n\eta_{11}}\times$$
$$\times\left[\in_{11}(1-\beta^n(1+P)^n)+\in_{12}(1-\beta^n)-\frac{1}{r}\right]+B\,, \tag{12}$$

where: B is any constant.

Applying logarithmic differentiation in Eq.(12) and using Eq.(10), and then using $P\to\pm\infty$, we get

$$R=AC_3r^{C_1}e^{C_2r^{-k}}\,,\quad c_1=\frac{(m-k+1)C_{011}+2C_{066}}{\frac{e_{11}^2}{\eta_{11}}-C_{011}}\,,$$

$$\text{and}\quad c_2=\frac{\frac{e_{11}^2}{\eta_{11}}(m+1)}{\left(\frac{e_{11}^2}{\eta_{11}}-C_{011}\right)b^{-k}}\,. \tag{13}$$

The stresses evaluated using Eqs.(13) and (8), are given

$$T_{rr}=AC_3r^{C_1}e^{C_2r^{-k}}-B-\beta_1\theta\,, \tag{14}$$

$$T_{\theta\theta}=(m+1)C_3r^{C_1}e^{C_2r^{-k}}+C_3C_1r^{C_1}e^{C_2r^{-k}}-(\alpha_1C_{011}+2\alpha_2C_{012})\left(\frac{r}{b}\right)^k\times$$
$$\times\theta_0\left(\frac{\log(r/b)}{r\log(a/b)}+\frac{1}{r\log(a/b)}\right)-kC_3C_2r^{C_1-k}e^{C_2r^{-k}}+\rho_0r^2\omega^2\left(\frac{r}{b}\right)^t.$$

Using boundary conditions of Eq.(11) in Eq.(14) we have

$$B=\frac{-p_1+(\alpha_1C_{011}+2\alpha_1C_{012})\left(\frac{a}{b}\right)^k\theta}{a^{C_1}e^{C_2a^{-k}}-b^{C_1}e^{C_2b^{-k}}}b^{C_1}e^{C_2b^{-k}}\,,$$

$$C_3=\frac{-p_1+(\alpha_1C_{011}+2\alpha_1C_{012})\left(\frac{a}{b}\right)^k\theta}{a^{C_1}e^{C_2a^{-k}}-b^{C_1}e^{C_2b^{-k}}}\,. \tag{15}$$

Yielding criterion is taken as $|T_{rr}-T_{\theta\theta}|_{r=a}=$

$$=\left|-(m+1)C_3a^{C_1}e^{C_2a^{-k}}-B+(\alpha_1C_{011}+2\alpha_2C_{012})\theta_0\left[\left(\frac{a}{b}\right)^{k-1-m}-\left(\frac{a}{b}\right)^k+\frac{1}{a\log(a/b)}\right]-kC_3C_2a^{C_1-k}e^{C_2a^{-k}}-\rho_0a^2\omega^2\left(\frac{a}{b}\right)^t\right|=\gamma_1\,. \tag{16}$$

Pressure needed for initial yielding is given by

$$p_i=\frac{p}{\gamma_1}=\frac{a^{C_1}e^{C_2a^{-k}}-b^{C_1}e^{C_2b^{-k}}}{ma^{C_1}e^{C_2b^{-k}}+b^{C_1}e^{C_2b^{-k}}}\left\{1+\frac{(\alpha_1C_{011}+2\alpha_1C_{012})\left(\frac{a}{b}\right)^k\left(ma^{C_1}e^{C_2b^{-k}}-b^{C_1}e^{C_2b^{-k}}\right)\theta_0}{a^{C_1}e^{C_2b^{-k}}-b^{C_1}e^{C_2b^{-k}}}+(\alpha_1C_{011}+2\alpha_1C_{012})\times\right.$$
$$\left.\times\left(\left(\frac{a}{b}\right)^{k-m-1}-\left(\frac{a}{b}\right)^k+\frac{1}{a\log(a/b)}\right)\left(\frac{a}{b}\right)^k+\frac{\rho_0a^2\omega^2}{\gamma_1}\left(\frac{a}{b}\right)^t\right\}. \tag{17}$$

Absolutely plastic state happens at the external surface. Consequently $|T_{rr}-T_{\theta\theta}|$ from Eqs.(14) at $r=b$,

$$|T_{rr}-T_{\theta\theta}|_{r=b}=\left|-(m+1)C_3b^{C_1}e^{C_2b^{-k}}-B+(\alpha_1C_{011}+2\alpha_2C_{012})\theta_0\frac{1}{b\log(a/b)}-kC_3C_2b^{C_1-k}e^{C_2b^{-k}}-\rho_0b^2\omega^2\right|=\gamma_2\,. \tag{18}$$

Pressure needed for absolutely plastic state is given by

$$p_f=\frac{p}{\gamma_2}=\frac{(a/b)^{C'_1}e^{C'_2a^{-k}}-e^{C'_2b^{-k}}}{m(a/b)^{C'_1}e^{C'_2b^{-k}}+e^{C'_2b^{-k}}}\left\{1+\frac{(\alpha_1C_{011}+2\alpha_2C_{012})(a/b)^k\left(ma^{C'_1}e^{C'_2b^{-k}}-b^{C'_1}e^{C'_2b^{-k}}\right)\theta_0}{R_0^{C'_1}e^{C'_2b^{-k}}-e^{C'_2b^{-k}}}+(\alpha_1C_{011}+2\alpha_2C_{012})\times\right.$$
$$\left.\times\left((a/b)^{k-m-1}-(a/b)^k+\frac{1}{a\log(a/b)}\right)(a/b)^k+\Omega_1R_0^{t+2}\right\}, \tag{19}$$

where: $C'_1=\dfrac{m-k+1}{(e_{11}^2/C_{011}\eta_{11})-1}$; and $C'_2=b^k(m+1)$.

Components assumed in non-dimensional form are as follows

$$R=\frac{r}{b},\quad R_0=\frac{a}{b},\quad \sigma_r=\frac{T_{rr}}{\gamma_1},\quad \sigma_\theta=\frac{T_{\theta\theta}}{\gamma_1},\quad p_i=\frac{p}{\gamma_1},\quad p_f=\frac{p}{\gamma_2},\quad \Omega_1=\frac{\rho_0 b^2\omega^2}{\gamma_1},\quad \Omega_2=\frac{\rho_0 b^2\omega^2}{\gamma_2}. \tag{20}$$

Using Eqs.(14) and (20), stresses in non-dimensional form are

$$\sigma_r=\frac{T_{rr}}{\gamma_1}=(\alpha_1C_{011}+2\alpha_1C_{012})(R)^k\frac{\theta\log(R_0)}{\log(R)}-\frac{-p_i+(\alpha_1C_{011}+2\alpha_2C_{012})(R_0)^k\theta}{a^{C_1}e^{C_2(R_0b)^{-k}}-b^{C_1}e^{C_2b^{-k}}}e^{C_2b^{-k}},$$

$$\sigma_\theta=\frac{T_{\theta\theta}}{\gamma_1}=\frac{(m+1+C_1-kC_2b^{-k}R^{-k})e^{C_2b^{-k}}(bR)^{C_1}(-p_i+(\alpha_1C_{011}+2\alpha_2C_{012}))(R_0)^k\theta}{(R_0^{C_1}e^{C_2(R_0b)-k}-e^{C_2b^{-k}})}-(\alpha_1C_{011}+2\alpha_2C_{012})\times$$
$$\times\left[(m+k+1)(R)^k\frac{\theta\log(R)}{\log(R_0)}+(R)^k\frac{\theta}{\log(R_0)}\right]+(R)^{t+2}\Omega_1. \tag{21}$$

Pressure needed for initial yielding in non - dimensional form is given by

$$p_i=\frac{p}{\gamma_1}=\frac{a^{C_1}e^{C_2R_0^{-k}b^{-k}}-b^{C_1}e^{C_2b^{-k}}}{ma^{C_1}e^{C_2b^{-k}}+b^{C_1}e^{C_2b^{-k}}}\left\{\times1+\frac{(\alpha_1C_{011}+2\alpha_1C_{012})(R_0)^k(mR_0^{C_1}e^{C_2b^{-k}}-e^{C_2b^{-k}})\theta_0}{R_0^{C_1}e^{C_2b^{-k}}-e^{C_2b^{-k}}}+(\alpha_1C_{011}+2\alpha_1C_{012})\right.$$
$$\left.\times\left((R_0)^{k-m-1}-(R_0)^k+\frac{1}{bR_0\log(R_0)}\right)(R_0)^k+\Omega_2(R_0)^t\right\}, \tag{22}$$

where: $C_1=\dfrac{(m-k+1)+2C_{011}/C_{066}}{(e_{11}^2/C_{011}\eta_{11})-1}$; and $C_2=\dfrac{\frac{e_{11}^2}{\eta_{11}}(m+1)}{\left(\frac{e_{11}^2}{\eta_{11}}-C_{011}\right)b^{-k}}$.

Pressure required for fully plastic in non - dimensional form is given by

$$p_f=\frac{p}{\gamma_2}=\frac{a^{C'_1}e^{C'_2R_0^{-k}b^{-k}}-b^{C_1}e^{C_2b^{-k}}}{ma^{C'_1}e^{C'_2b^{-k}}+b^{C'_1}e^{C'_2b^{-k}}}\left\{1+\frac{(\alpha_1C_{011}+2\alpha_1C_{012})(R_0)^k(mR_0^{C'_1}e^{C'_2b^{-k}}-e^{C'_2b^{-k}})\theta_0}{R_0^{C'_1}e^{C'_2b^{-k}}-e^{C'_2b^{-k}}}+(\alpha_1C_{011}+2\alpha_1C_{012})\times\right.$$
$$\left.\times\left((R_0)^{k-m-1}-(R_0)^k+\frac{1}{bR_0\log(R_0)}\right)(R_0)^k+\Omega_2(R_0)^t\right\}, \tag{23}$$

where: $C'_1=\dfrac{m-k+1}{(e_{11}^2/C_{011}\eta_{11})-1}$; and $C'_2=b^k(m+1)$.

Fully plastic stresses in non-dimensional form are given by

$$\sigma_r=\frac{T_{rr}}{\gamma_1}=(\alpha_1C_{011}+2\alpha_1C_{012})(R)^k\frac{\theta\log(R_0)}{\log(R)}-\frac{-p_i+(\alpha_1C_{011}+2\alpha_2C_{012})(R_0)^k\theta}{a^{C'_1}e^{C'_2(R_0b)^{-k}}-b^{C'_1}e^{C'_2b^{-k}}}e^{C'_2b^{-k}},$$

$$\sigma_\theta=\frac{T_{\theta\theta}}{\gamma_1}=\frac{(m+1+C'_1-kC'_2b^{-k}R^{-k})e^{C'_2b^{-k}}(bR)^{C'_1}(-p_i+(\alpha_1C_{011}+2\alpha_2C_{012}))(R_0)^k\theta}{(R_0^{C'_1}e^{C_2(R_0b)^{-k}}-e^{C'_2b^{-k}})}-(\alpha_1C_{011}+2\alpha_2C_{012})\times$$
$$\times\left[(m+k+1)(R)^k\frac{\theta\log(R)}{\log(R_0)}+(R)^k\frac{\theta}{\log(R_0)}\right]+(R)^{t+2}\Omega_1, \tag{24}$$

where: $C'_1=\dfrac{m-k+1}{(e_{11}^2/C_{011}\eta_{11})-1}$; and $C'_2=b^k(m+1)$.

NUMERICAL CALCULATIONS AND DISCUSSION

PZT4 and $BaTiO_3$

Figures 1a and 1b illustrate pressure values on innermost surface of the transversely isotropic disc made of barium titanate ($BaTiO_3$) and PZT4 (piezoceramic) with thickness parameter t = 1, variable density parameter m = 1, temperature θ = 5, and angular velocity of 100 and 500, respectively. It may be observed that pressure value increases with increasing radii ratio up to the centre of the disk and it is further decreased with increasing value of radii ratio for k =1, 2, and 3, in case of both materials. Pressure value is maximal for k = 3. With the increasing value of thermal gradient θ = 10, the pressure value increases as illustrated in Figs. 2a and 2b. Internal pressure is higher for the transversely isotropic disk made of PZT4.

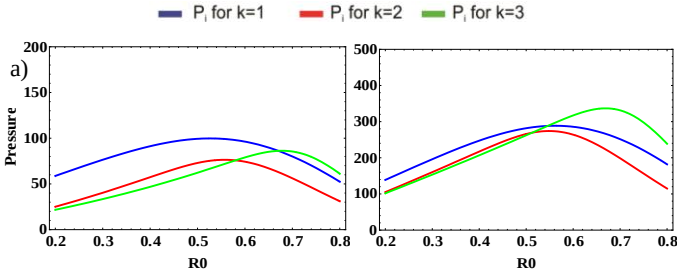

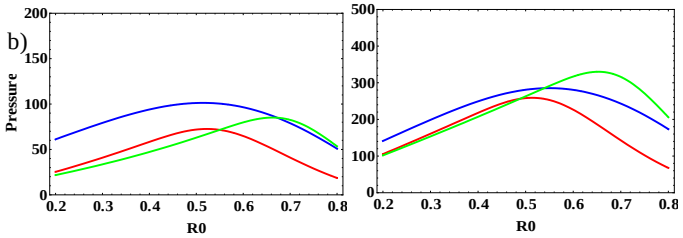

Figure 1. Internal pressure on $BaTiO_3$ and PZT4 with t =1, m =1, θ = 5, and angular velocity of a) 100; and b) 500.

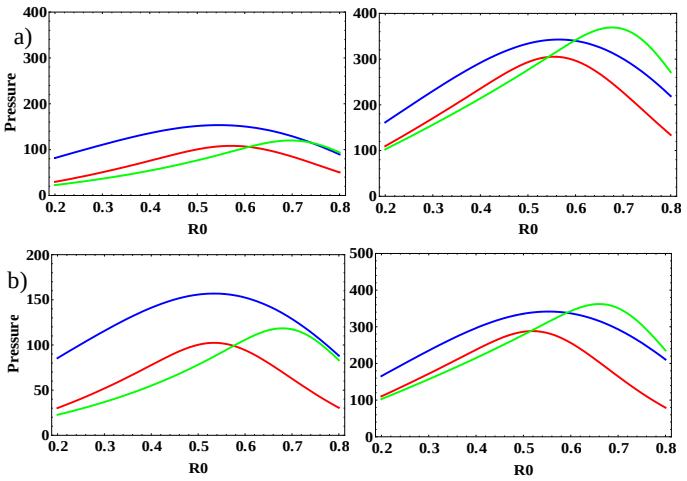

Figure 2. Internal pressure on $BaTiO_3$ and PZT4 with t = 1, m = 1, θ = 10, and angular velocity of a) 100; and b) 500.

Figures 3a and 3b show the plot of internal pressure with radii ratios for circular disk made of $BaTiO_3$ and PZT4 with thickness parameter t = 2, variable density parameter m = 2, temperature θ = 5, and angular velocity of 100 and 500, in respect. Pressure has minimal value at the innermost surface of the disk and maximal value at the outermost surface for k = 1, 2, and 3. Pressure values are further increasing with increasing value of temperature gradient (θ = 10), as illustrated in Figs. 4a and 4b. Internal pressure is higher for the transversely isotropic disk made of PZT4.

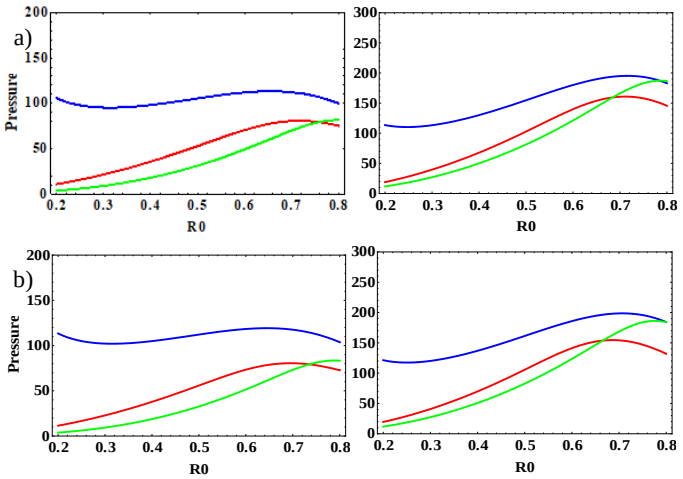

Figure 3. Internal pressure on $BaTiO_3$ and PZT4 with t = 2, m = 2, θ = 5, and angular velocity of a) 100; and b) 500.

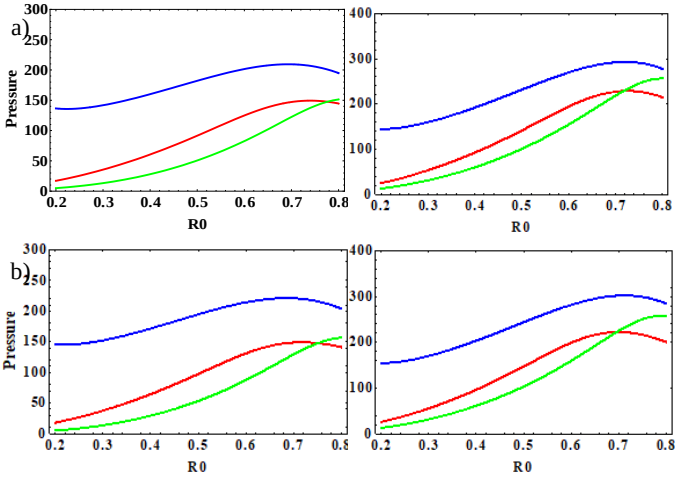

Figure 4. Internal pressure on $BaTiO_3$ and PZT4 with t = 2, m = 2, θ = 10, and angular velocity of a) 100; and b) 500.

Figures 5a and 5b demonstrate plots of pressure values in absolutely plastic state for the transversely isotropic disk of $BaTiO_3$ and PZT4 with thickness parameter t = 1, variable density parameter m = 1, temperature θ = 5, and angular velocity of 100 and 500, respectively. Pressure in absolutely plastic state achieves its maximal value at the centre of the disk for k = 1, 2, and 3. Pressure values are further increasing with increasing value of temperature gradient (θ = 10) as illustrated in Figs. 6a and 6b. Pressure in absolutely plastic state is higher for the transversely isotropic disk of PZT4.

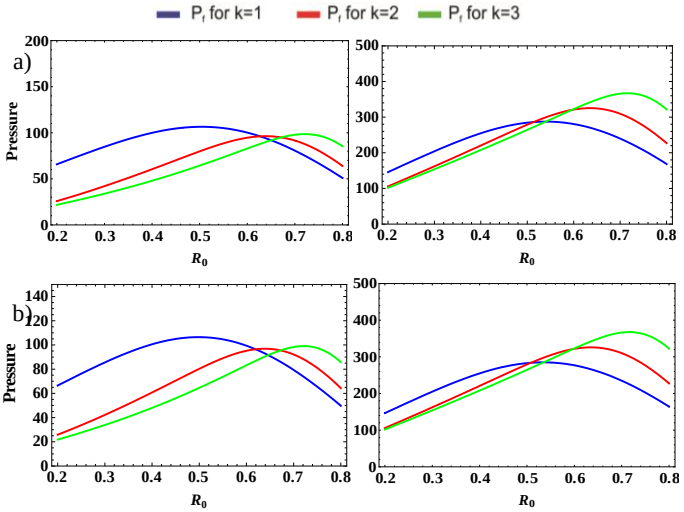

Figure 5. Fully plastic pressure of $BaTiO_3$ and PZT4 with t = 1, m = 1, θ = 5, and angular velocity of a) 100; and b) 500.

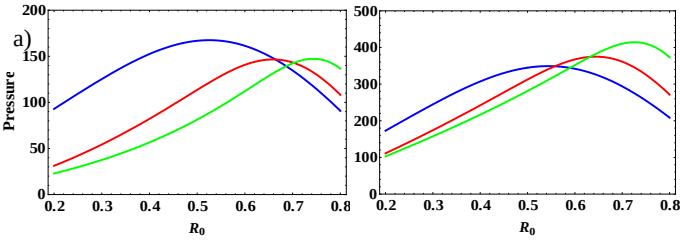

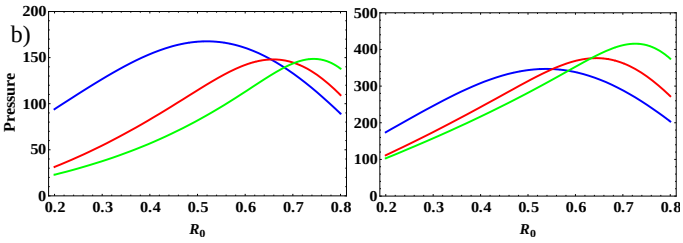

Figure 6. Fully plastic pressure of $BaTiO_3$ and PZT4 with t =1, m = 1, θ = 10, and angular velocity of a) 100; and b) 500.

Figures 7a and 7b show plots of pressure values in fully plastic state for transversely isotropic disk of $BaTiO_3$ and PZT4 with thickness parameter t = 2, variable density parameter m = 2, temperature θ = 5, and angular velocity of 100 and 500, in respect. Pressure in fully plastic state achieves its maximal value at the outermost surface of the disk for k = 1, 2, and 3. Pressure values are getting larger with the increment in temperature gradient (θ = 10) as illustrated in Figs. 8a and 8b. Pressure in absolutely plastic state is higher for the transversely isotropic disc of PZT4.

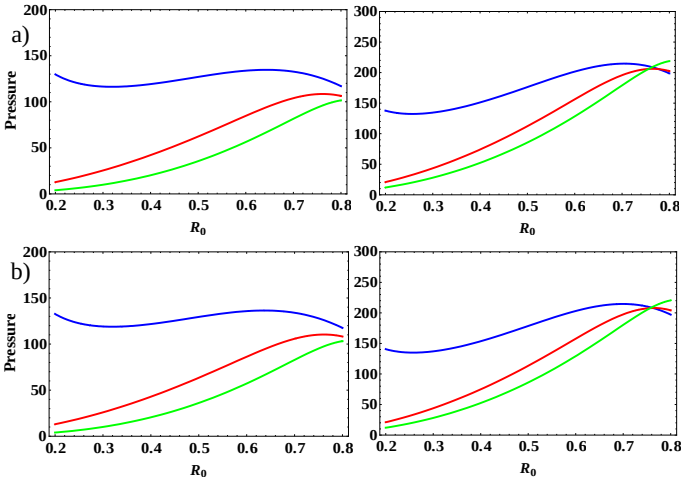

Figure 7. Fully plastic pressure of $BaTiO_3$ and PZT4 with t = 2, m = 2, θ = 5, and angular velocity of a) 100; and b) 500.

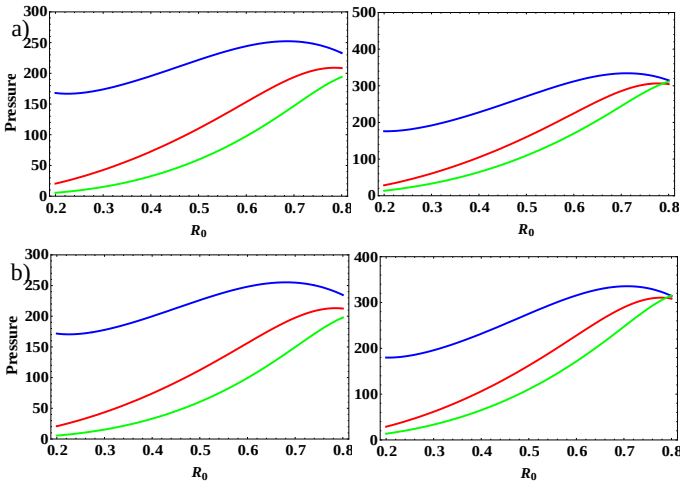

Figure 8. Fully plastic pressure of $BaTiO_3$ and PZT4 with t = 2, m = 2, θ = 10, and angular velocity of a) 100; and b) 500.

Transitional stresses

Figures 9a and 9b show the plot of transitional stresses with radii ratios for the transversely isotropic disk of $BaTiO_3$ and PZT4 with thickness parameter t = 1, variable density parameter m = 1, temperature θ = 5, and angular velocity of 100 and 500, respectively. It may be noted that transitional stresses are tensile in nature and increasing with radii ratio and achieve their maximum at outermost surface of the diskc for k = 1, 2, and 3, in case of both materials. With the increasing value of thermal gradient θ = 10, the values of transitional stresses increase as illustrated in Figs. 10a and 10b. Transitional stresses are higher for transversely isotropic disc made of PZT4.

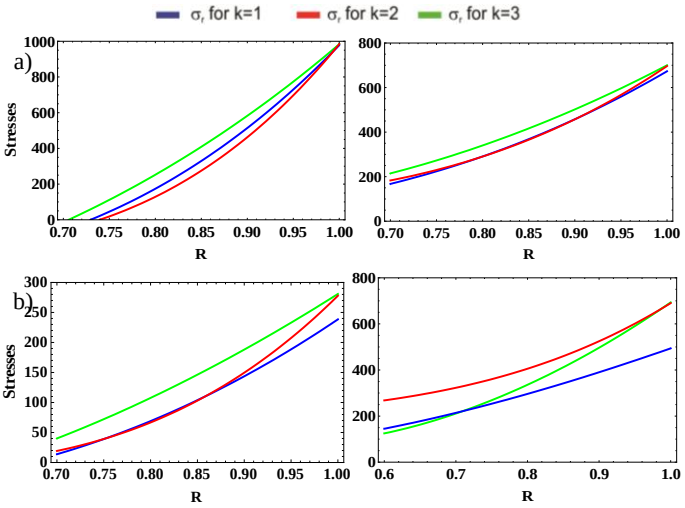

Figure 9. Transitional stresses for $BaTiO_3$ and PZT4 with t = 1, m = 1, θ = 5, and angular velocity of a) 100; and b) 500.

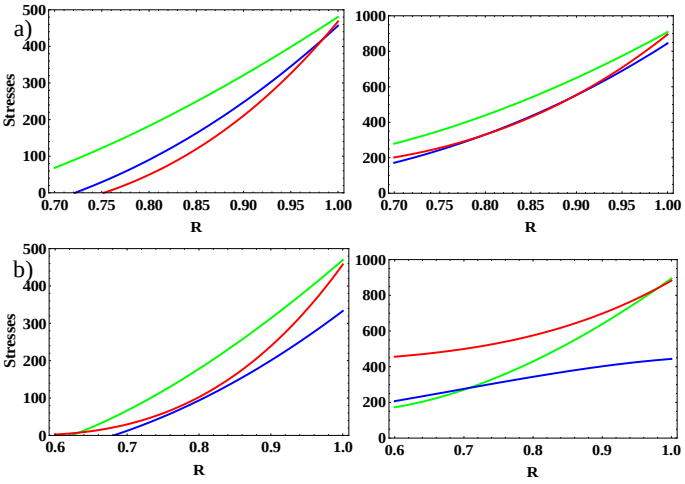

Figure 10. Transitional stresses for $BaTiO_3$ and PZT4 with t =1, m = 1, θ = 10, and angular velocity of a) 100; and b) 500.

Figures 11a and 11b show plots of transitional stresses with radii ratios for circular disk of $BaTiO_3$ and PZT4 with thickness parameter t = 2, variable density parameter m = 2, temperature θ = 5, and angular velocity of 100 and 500, in respect. Transitional stresses have maximal value at the outer surface of the disk for k = 1, 2, and 3. With increasing value of thermal gradient θ = 10 , the value of transitional stresses increases as illustrated in Figs. 12a and 12b. Transitional

stresses are higher for the transversely isotropic disk made of PZT4.

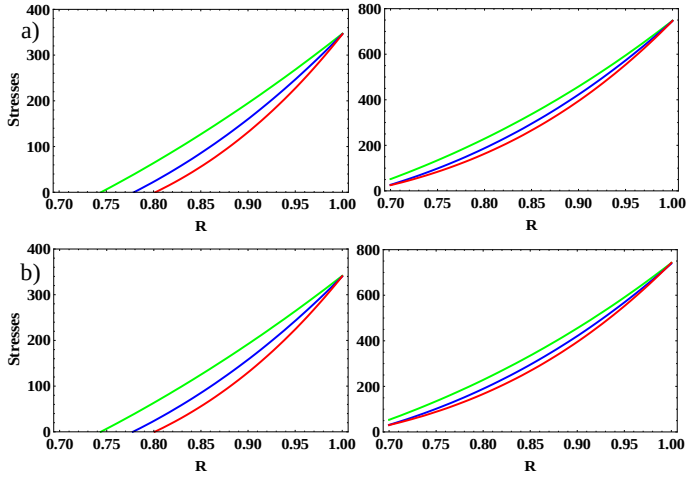

Figure 11. Transitional stresses for $BaTiO_3$ and PZT4 with t = 2, m = 2, θ = 5, and angular velocity of a) 100; and b) 500.

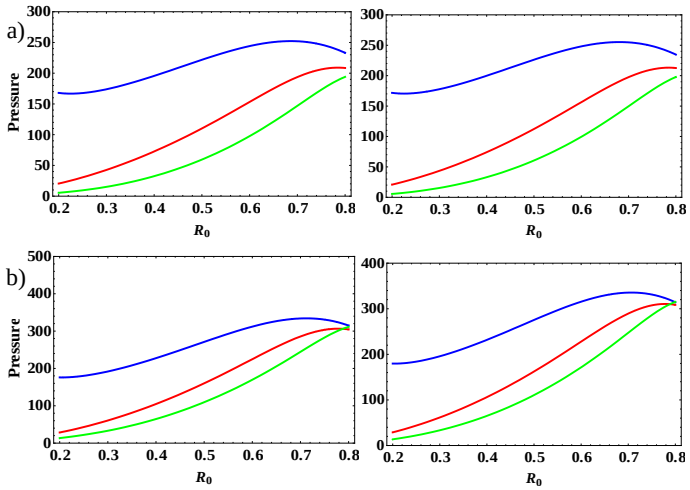

Figure 12. Transitional stresses for $BaTiO_3$ and PZT4 with t = 2, m = 2, θ = 10, and angular velocity of a) 100; and b) 500.

Fully plastic stresses

Figures 13a and 13b show plots of absolutely plastic stresses with radii ratios for circular disk of $BaTiO_3$ and PZT4 with thickness parameter t = 1, variable density parameter m = 1, temperature θ = 5, and angular velocity of 100 and 500, respectively. Transitional stresses are tensile in nature and increasing with radii ratio and achieve largest value at the outermost surface of the disk for k = 1, 2, and 3. With the increasing value of thermal gradient θ = 10, the value of transitional stresses increases as illustrated in Figs. 14a and 14b. Fully plastic stresses are higher for transversely isotropic disc made of PZT4.

Figures 15a and 15b show plots of fully plastic stresses with radii ratios for circular disk of $BaTiO_3$ and PZT4 with thickness parameter t = 2, variable density parameter m = 2, temperature θ = 5, and angular velocity of 100 and 500, in respect. Transitional stresses are tensile in nature and increasing with radii ratio and achieve the largest value at the outermost surface of the disk for k = 1, 2, and 3. With the increasing value of thermal gradient θ = 10, the value of transitional stresses increases as illustrated in Figs. 16a and 16b. Fully plastic stresses are higher for the transversely isotropic disc made of PZT4.

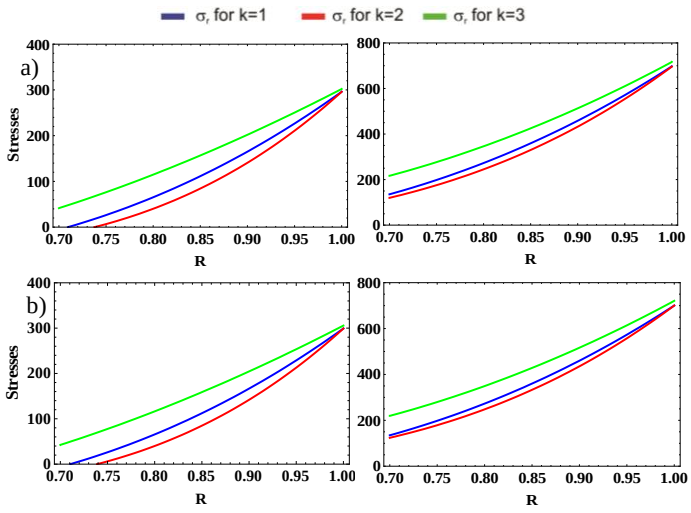

Figure 13. Fully plastic stresses for $BaTiO_3$ and PZT4 with t = 1, m =1, θ = 5, and angular velocity of a) 100; and b) 500.

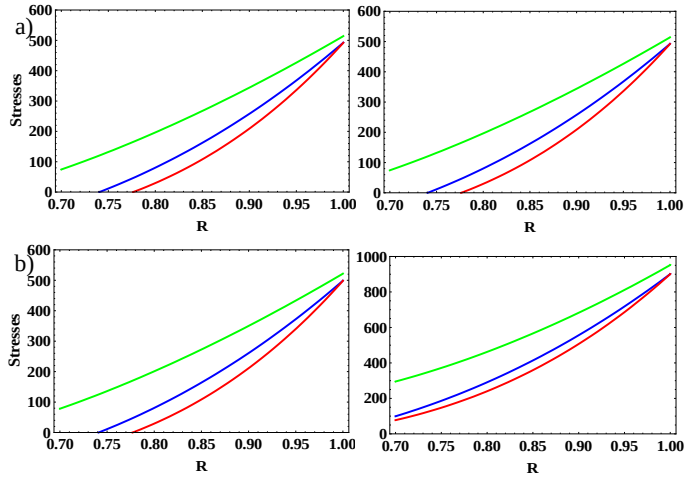

Figure 14. Fully plastic stresses for $BaTiO_3$ and PZT4 with t = 1, m =1, θ = 10, and angular velocity of a) 100; and b) 500.

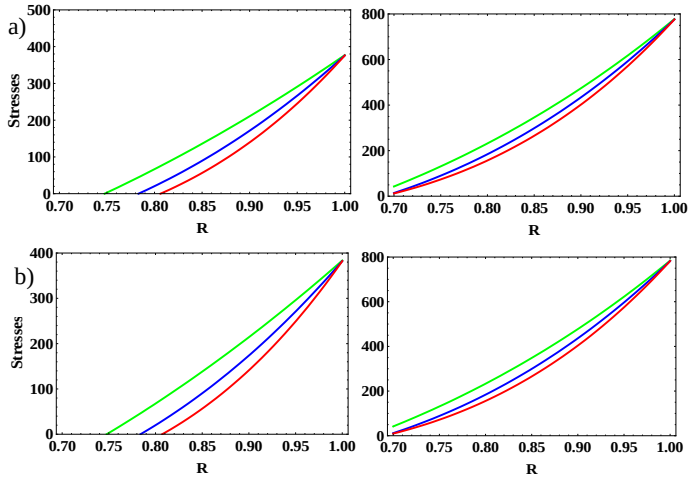

Figure 15. Fully plastic stresses for $BaTiO_3$ and PZT4 with t = 2, m =2, θ = 5, and angular velocity of a) 100; and b) 500.

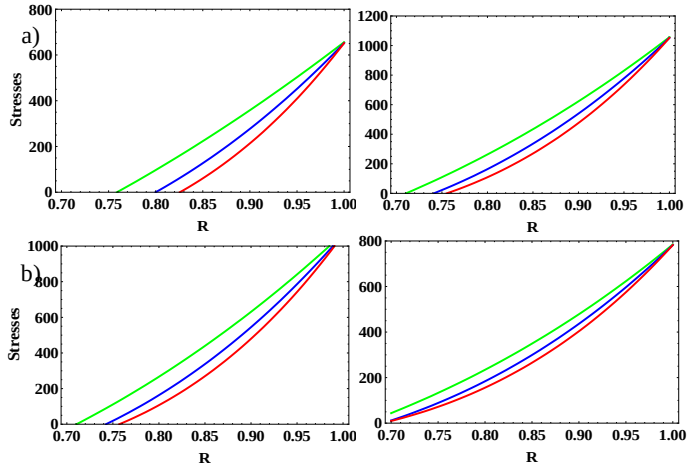

Figure 16. Fully plastic stresses for $BaTiO_3$ and PZT4 with t = 2, m =2, θ = 10, and angular velocity of a) 100; and b) 500.

CONCLUSION

Studied here is the deformation in a thin circular disk made of $BaTiO_3$ and PZT4, due to angular velocity, temperature and pressure. In the present research, the components of transitional stresses are obtained and shown graphically to depict the effects of rotation, pressure, and temperature. There is significant impact of rotation and temperature on stresses for transversely isotropic rotating disk made of barium titanate ($BaTiO_3$) and PZT4 (piezoceramic). With increase in rotation and temperature, the circumferential stresses further increase significantly. It is concluded on the basis of all the calculations and results that the disk of piezoelectric material $BaTiO_3$ is better than the disk made of piezoceramic material PZT4. Parameters obtained from this research can be used to design pressure sensors, radar antennae, and many other devices, also machines, or structures, in engineering applications.

REFERENCES

1. Nguyen, L.B., Nguyen, N.V., Thai, C.H., et al. (2019), *An isogeometric Bézier finite element analysis for piezoelectric FG porous plates reinforced by graphene platelets*, Compos. Struct. 214: 227-245. doi: 10.1016/j.compstruct.2019.01.077
2. Barati, M.R., Shahverdi, H., Zenkour, A.M. (2017), *Electro-mechanical vibration of smart piezoelectric FG plates with porosities according to a refined four-variable theory*, Mech. Adv. Mater. Struct. 24(12): 987-998. doi: 10.1080/15376494.2016.1196799
3. Nguyen, N.V., Lee, J., Nguyen-Xuan, H. (2019), *Active vibration control of GPLs-reinforced FG metal foam plates with piezoelectric sensor and actuator layers*, Compos. Part B: Eng. 172: 769-784. doi: 10.1016/j.compositesb.2019.05.060
4. Zharfi, H., Ekhteraei Toussi, H. (2018), *Time dependent creep analysis in thick FGM rotating disk with two-dimensional pattern of heterogeneity*, Int. J Mech. Sci. 140(1): 351-360.
5. Khanna, K., Gupta, V.K., Nigam, S.P. (2017), *Creep analysis in functionally graded rotating disc using Tresca criterion and comparison with von-Mises criterion*, Mater. Today Proceed. 4(2)A: 2431-2438. doi: 10.1016/j.matpr.2017.02.094
6. Dai, H.-L., Dai, T., Zheng, H.-Y. (2012), *Stresses distributions in a rotating functionally graded piezoelectric hollow cylinder*, Meccanica, 47(2): 423-436. doi: 10.1007/s11012-011-9447-8
7. Jafari Fesharaki, J., Jafari Fesharaki, V., Yazdipoor, M., Razavian, B. (2012), *Two-dimensional solution for electro-mechanical behavior of functionally graded piezoelectric hollow cylinder*, Appl. Math. Model. 36(11): 5521-5533. doi: 10.1016/j.apm.2012.01.019
8. Akbarzadeh, A.H., Abbasi, M., Hosseini Zad, S.K., Eslami, M. R. (2011), *Dynamic analysis of functionally graded plates using the hybrid Fourier-Laplace transform under thermomechanical loading*. Meccanica, 46(7): 1373-1392. doi: 10.1007/s11012-010-9397-6
9. Borah, B.N. (2005), *Thermo-elastic-plastic transition*, Contemp. Math. 379: 93-111.
10. Sharma, S., Sahni, M. (2009), *Elastic-plastic transition of transversely isotropic thin rotating disc*, Contemp. Eng. Sci. 2(9): 433-440.
11. Aggarwal, A.K., Sharma, R., Sharma, S. (2013), *Safety analysis using Lebesgue strain measure of thick-walled cylinder for functionally graded material under internal and external pressure*, The Sci. World J, 2013: Art. ID. 676190. doi: 10.1155/2013/676190
12. Sharma, S., Sahai, I., Kumar, R. (2013), *Creep transition of a thin rotating annular disk of exponentially variable thickness with inclusion and edge load*, Procedia Eng. 55: 348-354. doi: 10.1016/j.proeng.2013.03.264
13. Aggarwal, A.K., Sharma, R., Sharma, S. (2014), *Collapse pressure analysis of transversely isotropic thick-walled cylinder using Lebesgue strain measure and transition theory*, The Sci. World J, 2014, Art ID. 240954. doi: 10.1155/2014/240954
14. Sharma, S., Yadav, S., Sharma, R. (2017), *Thermal creep analysis of functionally graded thick-walled cylinder subjected to torsion and internal and external pressure*, J Solid Mech. 9(2): 302-318.
15. Sharma, S., Panchal, R. (2017), *Thermal creep deformation in pressurized thick-walled functionally graded rotating spherical shell*, Int. J Pure Appl. Math. 114(3): 435-444. doi: 10.12732/ijpam.v114i3.2
16. Sharma, S., Sharma, R., Panchal, R. (2018), *Creep transition in transversely isotropic composite circular cylinder subjected to internal pressure*, Int. J Pure Appl. Math. 120(1): 87-96. doi: 10.12732/ ijpam.v120i1.8
17. Sharma, S., Yadav, S., Sharma, R. (2018), *Creep torsion in thick-walled circular cylinder under internal and external pressure*, Struct. Integ. Life, 18(2): 89-97.
18. Sharma, R., Sahni, M. (2020), *Analysis of creep stresses in thin rotating disc composed of piezoelectric material*, Struct. Integ. Life, Vol.20, Special Issue : S45-S49.
19. Sharma, S., Panchal, R. (2018), *Creep stresses in functionally graded rotating orthotropic cylinder with varying thickness and density under internal and external pressure*, Struct. Integ. Life, 18(2): 111-119.
20. Yadav, S., Sharma, S. (2018), *Torsion in microstructure hollow thick-walled circular cylinder made up of orthotropic material*, J Solid Mech. 10(3): 581-590.
21. Sharma, S., Panchal, R. (2018), *Elastic-plastic transition of pressurized functionally graded orthotropic cylinder using Seth's transition theory*, J Solid Mech. 10(2): 450-463.
22. Sharma, R., Sharma, S., Radaković, Z. (2018), *Thermal creep analysis of pressurized thick-walled cylindrical vessels*, Struct. Integ. Life, 18(1): 7-14.
23. Sharma, S., Yadav, S., Radaković, Z. (2018), *Finite creep deformation in thick-walled circular cylinder with varying compressibility under external pressure*, Struct. Integ. Life, 18(1): 31-36.
24. Sharma, S., Yadav, S. (2019), *Numerical solution of thermal elastic-plastic functionally graded thin rotating disk with exponentially variable thickness and variable density*, Thermal Sci. 23(1): 125-136. doi: 10.2298/TSCI131001136S